Mechanistic feature-scale profile simulation of SiO_2 LPCVD by TEOS pyrolysis

Andrew H. Labun
Intel Corporation, 5200 NE Elam Young Parkway, Hillsboro, OR 97124-6497

Harry K. Moffat
Sandia National Laboratories, Albuquerque, NM 87185

Timothy S. Cale
Dept. of Chemical Engineering, School of Engineering, Rensselaer Polytechnic Institute, 110 8th Street, Troy, NY 12180-3590

DISCLAIMER

DISCLAIMER

Portions of this document may be illegible in electronic image products. Images are produced from the best available original document.

ABSTRACT

Simulation of chemical vapor deposition (CVD) in submicron features typical of semiconductor devices has been facilitated by extending the EVOLVE thin film etch and deposition simulation code to use thermal reaction mechanisms expressed in the Chemkin format. This allows consistent coupling between EVOLVE and reactor simulation codes that use Chemkin. In an application of a reactor-scale simulation code providing surface fluxes to a feature-scale simulation code, a proposed reaction mechanism for TEOS pyrolysis to deposit SiO_2, which had been applied successfully to reactor-scale simulation, is seen not to predict the low step coverage over trenches observed under short reactor residence time conditions. An apparent discrepancy between the mechanism and profile-evolution observations is a reduced degree of sensitivity of the deposition rate to the presence of reaction products, i.e., the byproduct inhibition effect is underpredicted. The cause of the proposed mechanism's insensitivity to byproduct inhibition is investigated with the combined reactor and topography simulators first by manipulating the surface to volume ratio of a simulated reactor and second by calibrating parameters in the proposed mechanism such as the calculated free energies of surface molecules. The conclusion is that the byproduct inhibition can not be enhanced to fit profile evolution data without comprising agreement with reactor scale data by simply adjusting mechanism parameters. Thus, additional surface reaction channels seem to be required to reproduce simultaneously experimental reactor-scale growth rates and experimental step coverages.

I. INTRODUCTION

A. Integration of Surface Chemkin into EVOLVE

Simulation of chemical vapor deposition (CVD) of thin films over submicron features is used in semiconductor manufacturing to either predict film thickness variation over feature topography or to analyze the physical or chemical processes involved in the deposition process. A common approach to simulating thickness variation is to assume that the CVD film's profile can be modeled by the deposition of a single, rate-limiting precursor species from the gas phase with first order reaction kinetics, using a calibrated sticking coefficient with a constant value[1]. This "single sticking coefficient" (SSC) approach offers the benefits of being tractable mathematically and of being conceptually simple. However, the SSC model does not use information about the complex surface kinetics of the CVD chemistries to which it is often applied. Thus, even for cases for which a given film profile can be matched using an SSC model, it will not be capable of making correct predictions about step coverage variation for conditions or geometries not similar to those used to make the calibrating sample. For more general prediction and analysis, a CVD topography simulation should use detailed descriptions of chemical reactions, usually in conjunction with a reactor-scale simulation to compute gas transport to and from the reactive surface and with chemical reaction rates and thermodynamic properties of species obtained by experiment and/or by calculation.

This paper describes feature-scale numerical simulation of a widely used CVD process using a system of reversible elementary chemical reactions implemented in a general purpose topography simulator, EVOLVE 5.0[2]; using the Chemkin[3] and Surface Chemkin[4] chemical kinetics reaction descriptions. The implementation of Chemkin within EVOLVE is described in Appendix A. Chemkin and Surface Chemkin software (hereafter referred to as "Chemkin") comprise a thermodynamics database for many molecules, interpreters to transform user-defined, human-readable chemical reaction mechanisms into a rate equation form suitable for numerical calculation, and subroutine libraries to perform kinetics calculations within simulation codes. EVOLVE applies gas transport calculations and mechanistic descriptions of reactions on surfaces to thin film etch and deposition over complex topography. Their combination makes calculation of the topography evolution of a broad class of CVD processes more convenient than in the past.

The link between Chemkin and EVOLVE has two major implications. First, a wide range of chemical reaction systems already expressed in the Chemkin formalism can be immediately simulated both at the reactor scale, using several Chemkin-based reactor simulation codes[5], and at the feature scale, using EVOLVE, *without manual reinterpretation of the reactions into a different reaction format.* This allows feature-scale simulators to employ detailed reaction mechanisms previously developed for the reactor scale. Second, computational analyses of deposition processes can be made at one length scale with immediate feedback to their consequences on other length scales. For instance, a predicted film profile inside a submicron feature will not only be sensitive to transport in the reactor and in the submicron feature, but also to the choice of homogeneous and heterogeneous reaction mechanisms. Feature- and reactor-scale models will test the validity of the mechanism at different time and length scales. A transport-reaction mechanism combination that may effectively predict conditions at one length scale may fail miserably when applied to another

length or time scale. In the current approach, the consequences of changes made to the Chemkin reaction mechanism files are automatically consistent in both the reactor simulators and EVOLVE. Thus, the addition of the feature-scale simulator to the existing suite of reactor-scale simulators allows CVD models to be tested more stringently against experiments and then to be applied more predictively than either the feature- or reactor-scale approach applied separately.

Although many projects may be addressed by EVOLVE when linked to a reactor simulator, including optimization of CVD processes for feature-scale film properties, the emphasis in this paper is on demonstrating the use of a topography simulation code in testing a detailed reaction mechanism. We evaluate a proposed reaction mechanism for the industrially significant thermal $Si(OC_2H_5)_4$ (TEOS) SiO_2 CVD process by comparing its step coverage prediction to experiment. We test the hypothesis that byproduct inhibition determines thin film step coverage in submicron trenches, and attempt the calibration of the surface reaction mechanism using step coverage information.

B. Step coverage in SiO_2 CVD by TEOS pyrolysis

The pyrolysis of TEOS to form SiO_2 is an example of a CVD process for which step coverage over submicron trenches has been studied experimentally and also simulated with both the SSC model as well as with models using more detailed kinetics.

We define the step coverage of a film deposited in a trench as the ratio of the film thickness at some location on the trench profile to the film thickness on the top, planar surface. The film thickness and hence the step coverage generally vary from one location on the trench profile to another. Unless otherwise stated, the step coverage on a sidewall at the height of the substrate's top, planar surface or at the trench bottom is intended when we speak of "the sidewall step coverage" or "the bottom step coverage."

Levin and Evans-Lutterodt[6] manipulated temperature, flow rate, and reactor pressure in a hot wall reactor. They found that the step coverage of SiO_2 films in trenches was higher when the total pressure increased for a constant TEOS flow rate, or when the flow rate was decreased for a constant total pressure. The step coverage was not influenced by temperature variations between 923 K and 1073 K. Their interpretation of these results was that gas-phase species which inhibited the surface reaction rate constant, and therefore led to an improvement in the step coverage, were produced at long residence times. Therefore, changes in reactor conditions leading to longer residence times such as an increase in reactor pressure or reduction in the total flow rate lead to better step coverage.

Becker *et al.*[7] performed depositions on 150 mm Si wafers mounted in standard wafer carriers in a horizontal furnace at temperatures between 923 and 1073 K and total pressures between 300 and 900 mTorr. Flow rates were kept constant leading to an increase in residence time with increased pressure. They observed that the reactor-scale deposition rate was a sublinearly increasing function of the total reactor pressure. They interpreted the sublinear behavior as evidence for inhibition of the surface reaction due to increased product gases. While the overall uniformity on wafers degraded (center-slow deposition) as the pressure increased, the bottom step coverage in high aspect ratio trenches (AR = 5) simultaneously improved from 53% to 78% with increased pressure.

Raupp *et al.* [8] reported the deposition rates and trench fills obtained in a cold wall reactor with a small heated sample under low residence time conditions. Their conditions were such that no reaction byproducts (including any reactive intermediate) in the reactor gas were expected. Their SiO_2 films had poor trench step coverages; e.g. 56% (sidewall) and 33% (bottom) in AR = 3.5 trenches.

Sorita *et al.*[9] studied TEOS gas-phase transport and reactions, attempting to decouple them using the so-called "micro/macrocavity method," a system of wafers patterned with trenches of various ARs, stacked with separations varying from 0.1 mm to ~3 mm, to discriminate the role of gaseous diffusion from that of surface kinetics. Their apparatus consisted of a 15 mm diameter hot wall tube with TEOS introduced through a N_2 bubbler. They raised the total pressure from 2 to 760 Torr by adding more N_2. Not only did they find that step coverage improved with increasing pressure (and hence residence time) but also that more closely spaced wafers led to improved step coverage at the centre. Uniformity suffered, however, as noted by Becker.

A common observation from the studies referenced above is that longer residence time and more closely spaced wafers lead to improved step coverage over trenches, but poorer film uniformity across closely spaced wafers.

C. Review of prior step-coverage models

Proposed models of the step coverage of the TEOS CVD process fall into two categories: those which use the SSC model with multiple species and those which use more complex surface reaction models.

Application of the SSC model to experimentally observed SiO_2 deposition step coverage trends is not straightforward. While TEOS itself decomposes on the SiO_2 surface, causing deposition, it is commonly accepted that a homogeneous reaction leads to an intermediate molecule which is a much more reactive deposition precursor species. Immediately, it becomes necessary to deal with more than one deposition precursor species. Thus, Islamraja *et al.*[10] demonstrated that, while the SSC model (presumably neglecting TEOS itself and treating the reactive intermediate gas species in a first-order deposition reaction) could fit a film profile of a nearly filled trench, it could not fit the profile corresponding to an earlier phase of the trench fill and it predicted a deposition rate orders of magnitude greater than that observed. However, the SSC model with *two* precursors with independent deposition channels could fit both the time evolution of the profile and the deposition rate. The TEOS molecule was assigned a sticking coefficient of 10^{-4} and the intermediate was assigned a sticking coefficient of 1. The improvement in step coverage and decline of deposition rate with pressure ran counter to their assumption of the formation of a highly reactive intermediate in the gas phase, so they proposed that excessive gaseous collisions depleted the intermediate. Despite allusions to chemistry in their work, their simple model did not identify particular species or reaction channels.

In their analysis of step coverage and deposition rate between their accurately spaced samples, Sorita *et al.*[9] added diffusive transport between wafers to the SSC. To explain their results at three pressures, they required three deposition species with different sticking coefficients. To explain the apparent contradiction between higher pressure (to make more of the supposed highly reactive

intermediates) and improved step coverage, they proposed that the diffusivity of the intermediates was so low that near atmospheric pressure the deposition was transport limited. However, Levin and Evans-Lutterodt's earlier results indicated that residence time at a given pressure was decisive in determining step coverage[6]. Because of their assumption of the SSC model, Sorita *et al.* did not consider the effects of byproduct inhibition on deposition rate or uniformity.

Instead of the SSC model, Raupp *et al.*[8] simulated deposition using the "byproduct inhibition" model, in which an unspecified gaseous product of heterogeneous decomposition of TEOS on the SiO_2 surface is readsorbed, blocking surface sites from further deposition reactions and reducing the reaction rate deep inside the feature. As used in the simulations, this simple mechanism was expressed in the form of a global rate expression rather than explicitly as a system of elementary step reactions. This model did indeed match the deposition profiles observed in their system when implemented in the EVOLVE topography simulator. Although they did not have experimental data on the relationship between residence time and step coverage, it is shown below that their model was consistent with observed residence time effects.

II. Proposed reaction mechanism for TEOS pyrolysis

A. Surface Chemkin reaction mechanism

Coltrin *et al.* [11] proposed what is termed here the "SNL" mechanism for TEOS pyrolysis, with reactions listed in Appendix B. The surface reactions are depicted schematically in Figure 1. It consists of both homogeneous and heterogeneous reactions; thermodynamic properties of gas and surface species obtained from the literature, from *ab initio* calculations, and from estimates[13]; and estimates of Leonard-Jones intermolecular force parameters needed for the calculation of transport properties based on dilute gas theory. Sticking coefficients for TEOS and triethoxysilanol ($Si(OH)(OC_2H_5)_3$) were calibrated to molecular beam experiments using Aurora, a perfectly-stirred reactor (PSR) simulator[14]. The remaining rate parameters and activation energies in their mechanism were fitted with Chemkin-based reactor simulation codes to reported CVD film deposition rates on flat wafer surfaces. The SNL mechanism quantitatively reproduced the horizontal furnace deposition rate results of Desu [15], among others, using Aurora as well as the OVEND horizontal wafer batch reactor simulator[16]. The mechanism includes the reversible beta-hydride decomposition of TEOS in the gas phase, principally to form triethoxysilanol and ethylene (C_2H_4). Triethoxysilanol is thus identified as the highly reactive intermediate mentioned earlier. Further reactions decomposing TEOS reaction byproducts are not included, since these were found to be insignificant in the reactor-scale simulations. Both TEOS and triethoxysilanol may chemisorb to sites on the reactive surface terminated by hydroxyl groups, releasing either ethanol (C_2H_5OH) or water (H_2O). Further reactions remove the ethoxy ligands (represented by the symbol E = OC_2H_5) from the adsorbates and create the glass bonds (represented by the symbol G = 0.5 O, such that SiG_4= SiO_2). This mechanism is applied in the present work to the problem of step coverage prediction using EVOLVE to simulate feature-scale transport and reactions.

B. Simulation of a step coverage experiment

Simulation of an existing, well-defined experiment is a useful means of testing a reaction mechanism. Unfortunately Levin and Evans-Lutterodt[6] and Becker *et al.*[7] provide insufficient

information, such as reactor dimensions, to reproduce their results via simulation. The apparatus of Sorita *et al.*[9] is too complex for simulation, also. Although the experiments reported in Raupp *et al.*[8] do not represent CVD process conditions (they used very low residence time and relatively cold gas), they provide full reactor and process information with a well-defined gas concentration owing to their simple flow pattern and use of a mass flow controller rather than a bubbler to deliver gaseous TEOS. The Chemkin-based MPSalsa[17] reactor code was used to simulate their experiment in two dimensions, using an axisymmetric geometry with the same volume and approximate configuration as their reactor. Figure 2 shows the geometry used in the simulation as well as the temperature field. The cold gas (T=300 K) that fills the bulk of the chamber is clearly visible, with the exception of a small heated boundary layer surrounding the heated Si sample (T=1023 K) and a plume of heated gas downstream of the sample. The boundary layer causes some TEOS decomposition, but its simulated fractional concentration remains above 99.99%, although that perhaps represents greater purity than that available in the bottle (see Figure 3). There is a flux of triethoxysilanol to the SiO_2 surface due to this boundary layer, amounting to $\sim 10^{-5}$ of the total flux to the surface and there are commensurate fluxes of the other product gases. Since triethoxysilanol is so highly reactive, it contributes ~20% of the total deposition even at its low mole fraction. Nonetheless, the TEOS channel dominates the deposition rate on the flat surface of the wafer.

MPSalsa predicts a deposition rate of 100 Å/min under these conditions, about three times the experimentally observed rate. However, the deposition rate measurements in Ref. 8 display scatter corresponding to approximately 50% uncertainty, so this discrepancy is not too alarming.

EVOLVE's gas concentration boundary condition was specified by the MPSalsa gas concentrations at a point on the sample surface. EVOLVE's simulated deposition rate on the flat surface of the sample was in agreement with the MPSalsa rate. However, the step coverage predicted by EVOLVE was 88% (bottom), not 33% as repoprted (Figure 4). This result has been confirmed independently in another topography simulator evaluating this same reaction mechanism[18]. There are at least two reasonable explanations for this discrepancy. The first is that the proposed reaction mechanism does not include some species and reactions that are important to step coverage. The second is that some parameters in the SNL mechanism do not have the appropriate values. Of course, both may be true. It is beyond the scope of this paper to propose additional species and reaction channels, but parameter values have been optimized using EVOLVE in the function call to an optimization program. It should be noted, however, that the deficiency in the reaction mechanism only became evident through the use of a topography simulation that uses the same chemical reaction mechanism as used in reactor simulations.

III. Reactor residence time effects on step coverage

The gas phase-based $Si(OH)(OC_2H_5)_3$ deposition channel, which dominates under normal CVD conditions, plays only a small part in the experimental conditions of Ref. 8. Thus, the overly conformal step coverage predicted by EVOLVE using the SNL mechanism for these experimental conditions may not necessarily be relevant to the observations of residence time effects in industrial CVD processes. However, the rest of the reaction mechanism, beyond the initial gas phase decomposition of TEOS, is the same. The simulated step coverage is insufficiently sensitive to byproduct inhibition for both Raupp's experimental conditions and for normal CVD conditions. By manipulating rate constants, however, the SNL mechanism can be made to display step

coverage improvement with increased residence time, demonstrating that this effect is a normal consequence of the decomposition of a large molecule with reactive gas byproducts in a small topographical feature.

A. Reactor-scale simulation

Aurora[14], a perfectly stirred reactor code based on Chemkin, was used to calculate the reactor-scale effects of residence time and provide gas fractions to EVOLVE for feature-scale simulations because of its rapid execution time. In addition to a Chemkin reaction mechanism (e.g. all the reactions in Table I), Aurora requires the user to specify only the reactor volume, surface area, gas and surface temperatures, input flow rate, pressure, and inlet gas fractions. As mentioned in the previous section, complete sets of these parameters for the step coverage experiments cited earlier could not be determined, except for that of Raupp *et al.* The values of these parameters for their experiment (except as noted below) are provided in Table II. Their experiment featured a very small reactive surface to *total* volume ratio relative to industrial CVD reactors. Of course, most of this total volume were irrelevant to the reaction on the hot surface; the low gas temperature prevented homogeneous reactions and virtually no gas byproducts were transported into this large volume because the fast flow swept them into the pump. Consequently, there were large gradients in composition. So their experiment had the transport attributes (such as flow rate) of a large, poorly-stirred volume but the reactive attributes of a small volume. Unfortunately, Aurora is not well-suited to reproducing this particular type of experiment.

However, Aurora can be used to simulate a related scenario, instructive for analyzing how the residence time affects step coverage. We define the temperature for the entire reactor volume in an Aurora simulation to be equal to the surface temperature, limit the surface area to the surface area of the sample, but use a relatively large volume (see Table III). These conditions simulate a hot wall reactor with no reactions on the walls, leading to an extremely small proportion of surface reaction byproducts in the gas but a large proportion of homogeneous reaction byproducts, whose concentration depends on the residence time. In contrast, surface reactions and byproduct inhibition dominate the kinetics of the interior of a submicron-sized trench or via feature. Thus, surface reaction byproducts have little effect on the deposition rates on the flat sample surface outside the feature, but have their maximum effect at the bottom of a high aspect ratio feature. This scenario amplifies the inhibitory effect of surface reaction byproducts on step coverage.

Aurora computed the steady-state reactor gas composition and film growth rates, and the rates of each reaction, for the scenario just described. Simulated residence time was controlled through the input gas flow rate, but because the number of moles of gas changes with flow rate due to reactions, there is no simple relationship between flow rate and residence time. Figure 5 shows that Aurora predicted deposition rates on the order of 0.1 $\mu m\ min^{-1}$, whereas Raupp *et al.*[8] reported deposition rates less than 0.01 $\mu m\ min^{-1}$. This difference is expected, since the experimental reactor's volume was almost completely filled with cold gas, whereas in Aurora, the entire volume is hot, leading to more production of the reactive intermediate, $Si(OH)(OC_2H_5)_3$.
Aurora's simulated gas composition is much more responsive to the residence time than the deposition rate is. For convenience, short (6.7 ms) and long residence time (372 ms) cases are designated to examine the effects of changes in gas composition. As the residence time increases from 6.7 ms to 372 ms, the TEOS fraction in the reactor drops to 28% of its low residence time value of 95%, while deposition rate declines to 72% of its low residence time value (Figure 5). The

reduction in TEOS fraction is accompanied by an increasing $SiG_3(OH)$ surface site fraction at the expense of all other surface species, which maintain their proportions while declining in absolute magnitude (Figure 6). Each species in the SNL mechanism occupies one site per molecule. The maximum SiO_2 deposition rate corresponds to the minimum $SiG_3(OH)$ surface site fraction.

B. Feature-scale simulation

EVOLVE used the gas fractions indicated in Figure 5 for the short and long residence time cases to calculate SiO_2 deposition rates and film profiles over a rectangular trench (AR=5). It is evident from Figure 7 that minimum step coverage indeed improves with lengthened residence time, ranging from 38% for short to 88% for long residence time, despite the increased fraction of $Si(OH)(OC_2H_5)_3$. The gas concentrations specified in the EVOLVE boundary conditions are the same as those in the volume of the PSR. So there is no transport effect which could limit $Si(OH)(OC_2H_5)_3$ concentrations at the surface. This demonstrates that the step coverage trend with residence time may be an effect of surface reaction kinetics alone.

Diagnostic graphs from EVOLVE help clarify how the step coverage trend arises. Figure 8 shows that the gas flux incident on the part of the surface within the trench can differ substantially from that on the top surface. The difference is most prominent for H_2O and C_2H_5OH in the short residence time case, where their fluxes to the surface are higher inside the trench by a factor of four. These gasses are generated by surface reactions, but their higher concentrations within the trench are associated with diminished deposition rates in the trench. Their presence inhibits one or more of the reaction steps in the mechanism.

Figure 9(a) shows a $SiG_3(OH)$ site fraction of ~70% under long residence time conditions, both inside and outside the trench, and all site fractions vary little over the feature. Figure 9(b) shows that, within the trench, the site fractions occupied by all surface species except $SiG_3(OH)$ decrease, indicating that the rates of reactions (B-5) and/or (B-12) have been slowed there. Conversely, outside the trench the $SiG_3(OH)$ site fraction is depressed to ~60% due to a dearth of the C_2H_5OH and/or H_2O needed to fuel the reverse reactions in (B-5) and (B-12).

Direct examination of the reaction rates (Figure 10) reveals that reaction (B-12) has been slowed, rather than reaction (B-5). The reduced rate of adsorption of $Si(OH)(OC_2H_5)_3$ limits the other reaction rates except for (B-5), whose rate of progress has increased.

It is also possible to view the difference between reactions inside and outside the trench in terms of the effective sticking probability $(\Gamma_{in} - \Gamma_{out})/\Gamma_{in}$ for each gas species, where Γ is defined as the flux. A negative effective sticking probability indicates that more of the gas species is being produced by the surface from surface reaction than is incident on the surface. Figure 11(a) shows that the only gas which is consumed at long residence time is $Si(OH)(OC_2H_5)_3$. Although $Si(OC_2H_5)_4$ is very nearly balanced between production and consumption, it is in net production on the entire surface but especially in the trench at long residence times. By contrast, at short residence time (Figure 11(b)), both $Si(OH)(OC_2H_5)_3$ and $Si(OC_2H_5)_4$ have a positive effective sticking probability. The effective sticking probability for $Si(OH)(OC_2H_5)_3$ declines by a factor of 3 in the trench, while the effective sticking probability for $Si(OC_2H_5)_4$ increases in the trench. The increase in the $SiG_3(OH)$

site fraction within the trench, which acts as a reactive site for TEOS chemisorption (B-5), is responsible for the increase in the $Si(OC_2H_5)_4$ sticking factor.

The residence time effects described above are manifestations of byproduct inhibition of reaction (B-12). Similar simulations were performed using larger surface/volume ratios. In those cases, not presented here, no significant trend in step coverage with residence time was seen, contrary to experiment. The significant amount of surface byproducts in those cases overwhelmed the weak residence time effect that can be produced by the mechanism as it stands.

IV. Mechanism calibration using EVOLVE

It is natural to attempt altering some parameter values in the proposed mechanism to improve agreement between predicted conformalities and the experiments reported by Raupp *et al.*[8] This is not merely motivated by a desire to improve the mechanism's predictions, but to see whether its *form* is adequate. That is, are additional or different reactions necessary or can satisfactory agreement between experiment and simulation be achieved with the current set using reasonable parameter values? Also, is byproduct inhibition the only mechanism capable of producing low step coverages, or could a forward reaction in either $Si(OC_2H_5)_4$ or $Si(OH)(OC_2H_5)_3$ within the existing form be a feasible rate-limiting step given altered parameters?

EVOLVE with Chemkin is well suited to iterative mechanism calibration schemes because it executes rapidly. EVOLVE's 2-D surface geometry is perfectly adequate for comparison to readily available trench and via topography data. Automatic parameter calibration of the selected parameters in the SNL mechanism was attempted based on the downhill simplex algorithm[19]. The parameters selected for adjustment were the free energies (at 1023 K) of the 5 surface species (via the standard entropy) and the forward rate coefficients of all the surface reactions except (B-5). This forward rate coefficient was a datum based on the molecular beam measurement, while the forward rate coefficients of (B-6), (B-7), and (B-8) were treated as fixed multiples of a common adjustable parameter, as explained in Ref. 11. There was thus a maximum of 10 adjustable parameters. Given a subset of n of the 10 parameters, a simplex of n+1 variations of the SNL mechanism was created by varying each parameter from the originally specified value in turn. Then the experiment reported by Raupp *et al.*[8] was "simulated" by setting Aurora's inlet gas fractions to the values specified in Table I. The flow rate was set very high, so that the outlet gas fractions didn't change significantly from their inlet values. The Aurora results were linked to EVOLVE, which then simulated deposition over an AR=3.5 trench. The resulting deposition rate and the sidewall and bottom step coverages were compared to experiment. A weighted sum of the squared differences between computed and experimental deposition rate and two step coverages was minimized by repeatedly choosing new parameter values according to the simplex algorithm and rerunning Aurora, etc. Convergence on a a set of parameter values was generally achieved after a few hundred iterations. Strictly, the calibration should use feedback between the reactor and topography simulation to achieve a consistent result, and ideally all available experiments would be calibrated simultaneously. However, it was not feasible to run the calibration loop with MPSalsa in it and Aurora was incapable of properly simulating the reactor, as mentioned earlier. Given the relatively minor role heterogeneous reactions are believed to play in determining the gas concentrations in the experiment, this non-self-consistent approach should still yield useful information.

The result of calibrating all 10 parameters is given in Table III. (Calibrations restricted to several smaller subsets of parameters did not yield successful fits to the experimental profile.) Considerable improvement in step coverage agreement has been achieved (see also Figure 4(b)), at the cost of worse deposition rate agreement. Although the new film profile matches experiment better and displays the observed characteristic that the film thickness along the trench interior is relatively uniform, the agreement is not completely satisfactory.

If this new film profile were an SSC or lumped reaction mechanism topography simulation result, success might be declared at this point. However, the detailed form of the reaction mechanism does not allow such an easy favorable conclusion. Calibration of what are ostensibly the actual kinetic or thermodynamic parameters must be reasonable for the result and the model to be plausible.What did the calibration do to the SNL mechanism to improve the step coverage agreement?

The behavior of the reaction mechanism after the calibration procedure may be understood by considering Figure 1 and the changes in the parameter values shown in Table V. First, the forward rate coefficients of (B-9) and (B-10) were reduced by four orders of magnitude. Simultaneously, the the free energy of SiG_3E was drastically reduced. Consequently, as seen in Figure 12, for the conditions of the simulation, reaction (B-11) tended wholly toward the forward direction and (B-9) and (B-10) toward equal forward and reverse reaction rates. These changes favor the generation of H_2O rather than C_2H_5OH as a deposition byproduct. The surfeit of H_2O forced $Si(OH)(OC_2H_5)_3$ into net production within the feature, slowing deposition there by creating a competitive etching reaction, and thus creating poor step coverage. This etching is an extreme case of byproduct inhibition.

It is not our belief that the SNL mechanism, as calibrated here, is better than the original. We do believe, however, that the mechanism lacks critical features such as additional reaction channels or surface species, which caused our fitting procedure to produce aphysical values for the entropies of surface species in an attempt at compensation. Moreover, the calibrated parameters significantly degraded the agreement of reactor-scale simulations with experiments such as those of Desu[15]. For example, where Desu reports in his Figure 3 a deposition rate of 16.5 nm/min for TEOS at 33.33 Pa and 1000 K and Aurora predicts 20 nm/min based on the original parameters[11], the calibrated parameters predicted only 4.2 nm/min[20].

V. CONCLUSIONS

Topography simulation is an important addition to the current methods used for developing chemical reaction mechanisms for CVD processes. The use of Chemkin in EVOLVE facilitates the testing of a reaction mechanism over the vastly different length scales provided by reactor-scale and feature-scale modeling. For the particular reaction mechanism studied, thermal TEOS deposition, we conclude that the reaction mechanism calibrated from reactor-scale data is inadequate to describe data produced from the feature-scale, and is therefore in need of revision.

ACKNOWLEDGEMENTS

The authors wish to acknowledge the many helpful conversations with and supplementary calculations performed for this paper by Drs. Pauline Ho and Michael E. Coltrin of Sandia National Laboratories, Albuquerque, New Mexico. Dr. Coltrin also contributed to the Chemkin extensions to EVOLVE 5.0 described in Appendix A. Sandia is a multiprogram laboratory operated by Sandia Corporation, a Lockheed Martin Company, for the United States Department of Energy under Contract DE-AC04-94AL85000.

Appendix A: Interpretation of Surface Chemkin mechanisms by EVOLVE

EVOLVE 5.0 has been extended, making it capable of transparently evaluating most CVD and etch mechanisms described by Surface Chemkin mechanism files. This allows EVOLVE to readily evaluate feature evolution corresponding to surface fluxes calculated by any Surface Chemkin-based reactor simulator.

Comparison of Mechanistic Rate Expressions

A rigorous description of the relationship between EVOLVE and Surface Chemkin requires a large number of symbols. The common nomenclature for EVOLVE and Surface Chemkin used below is adopted from Surface Chemkin documentation[4].

In both EVOLVE and Surface Chemkin, the I reversible (or irreversible) surface reactions involve K chemical species having stoichiometric coefficients ν_{ki} and chemical symbol χ_k and may be represented via the following formula:

$$\sum_{k=1}^{K} \nu'_{ki}\chi_k \Leftrightarrow \sum_{k=1}^{K} \nu''_{ki}\chi_k , \qquad 1 < i < I . \qquad \text{(A-1)}$$

The Surface Chemkin rate-of-progress variable for the i^{th} reaction q_i is equivalent to EVOLVE's *rate(j)* and is defined by the formula,

$$q_i = k_{fi} \prod_{k=1}^{K} [X_k]^{\nu'_{ki}} - k_{ri} \prod_{k=1}^{K} [X_k]^{\nu''_{ki}} , \qquad \text{(A-2)}$$

where k_{fi} and k_{ri} are the forward and reverse rate coefficients ($k_{fi} = AT^B\exp(C/RT)$), respectively, and $[X_k]$ is the activity of the k^{th} chemical species. Complications arise because the definitions of a chemical species' activity differ between EVOLVE and Surface Chemkin.

Fortunately for gasses and bulks, the relationship between variables in EVOLVE's *irtype*=4 rate expression and Eqn. (A-2) is straightforward. In both EVOLVE and Surface Chemkin, the activity of a gas is its molar concentration (mol cm^{-3}). Both EVOLVE and Chemkin support multiple materials with surface and bulk phases. EVOLVE implicitly considers the activity of bulk species to be unity, while Surface Chemkin requires the sum of the activities of bulk species in a single bulk phase to be unity. These two approaches are compatible as long as each bulk phase contains only one species. This is typical of CVD mechanisms and so it should not prove a burdensome restriction for most applications. Finally, Surface Chemkin does not treat physisorbed species as a special case, so the special treatment of physisorbed species in EVOLVE is not a concern.

However, the situation is more complicated for chemisorbed surface species. The composition of surface sites on the sth surface phase is given by an array of surface species site fractions Z_k. EVOLVE 5.0 only supports a single surface phase per material. This array is of length K_s. It is composed of N_s subunits of the site fractions of each of the species on a given site n. The site fractions on each site are normalized to sum to unity:

$$\sum_{k=K_f^s(n)}^{K_l^s(n)} Z_k(n) = 1. \qquad (n = N_f^s, \ldots, N_l^s) \qquad \text{(A-3)}$$

However, not all molecules adsorbed on the surface occupy a single site -- it is quite common for them to occupy multiple adjacent sites, either because they form more than one bond or cause steric hindrance because of their large size. Surface Chemkin uses a convention where the activity $[X_k]$ of a species on a surface phase with density of sites Γ_n (in moles/cm^2) is given by its species molar concentration

$$[X_k] = Z_k(n)\Gamma_n / \sigma_k(n), \tag{A-4}$$

where $\sigma_k(n)$ is the number of sites that each species k occupies. On the other hand, EVOLVE's *irtype*=4 rate expression uses a convention where the activity of a chemisorbed species (S_k) is given by its site molar concentration $Z_k(n)\Gamma_n$, related to $[X_k]$ by

$$[X_k] = S_k/\sigma_k(n). \tag{A-5}$$

The effect of this difference is that the forward and reverse rate coefficients in EVOLVE, and $\tilde{k}_{ri}$, are modified from their values in Surface Chemkin to account for the different activity conventions:

$$\tilde{k}_{fi} = k_{fi} \prod_{k=1}^{K} \sigma_k(n)^{-\nu'_{ki}} \quad \text{and} \quad \tilde{k}_{ri} = k_{ri} \prod_{k=1}^{K} \sigma_k(n)^{-\nu''_{ki}} \tag{A-6}$$

Sticking Coefficient Reaction Mechanisms

The so-called single sticking coefficient (SSC) model often assumed in topography simulation codes is a surrogate for chemical reaction rate expressions, usually justified on the grounds of ignorance of the true chemical mechanisms in film evolution. EVOLVE's *irtype*=1 implements a traditional SSC model where the sticking coefficient is the probability that a reactant molecule from the gas will react with the steady-state surface. Surface Chemkin also offers a STICK auxiliary keyword which makes its reactions into sticking coefficient reactions, but its "sticking coefficient" differs from that in EVOLVE. The Surface Chemkin sticking coefficient is the probability that a reaction involving a single gaseous reactant will proceed, and is modified by the surface fraction of the surface species (including vacancies) represented in the formula. Also, unlike the EVOLVE sticking coefficient reaction, the Surface Chemkin sticking coefficient reaction is in general reversible. Thus, the Surface Chemkin sticking coefficient is essentially just the conventional reaction rate (i.e. EVOLVE *irtype*=4) normalized by the incident flux of the reactant and the density of surface sites.

In fact, Surface Chemkin sticking coefficient reactions are interpreted by EVOLVE 5.0 as *irtype*=4 reactions. Surface Chemkin's sticking factor γ_i is related to k_{fi} by the formula

$$k_{fi} = \frac{\gamma_i}{(\Gamma_{tot})^m}\sqrt{\frac{RT}{2\pi W_k}} \tag{A-7}$$

where R is the universal gas constant, W_k is the molecular weight of the gas-phase species, Γ_{tot} is the total surface site concentration summed over all surface phases (number of moles of surface sites per unit area), and m is the sum of all the stoichiometric coefficients of reactants that are surface species.

In order to reproduce the behavior of a traditional-style (EVOLVE *irtype*=1) sticking coefficient reaction, simply make sure that no surface species appear in the reaction formula where a gas species transforms into a bulk species and that the reaction is irreversible.

APPENDIX B: TEOS CVD REACTION MECHANISM

The TEOS CVD reaction mechanism was proposed by Coltrin *et al.* [11] and includes four homogeneous and eight heterogeneous reactions. The homogeneous reactions are

$$Si(OC_2H_5)_4 \Leftrightarrow Si(OH)(OC_2H_5)_3 + C_2H_4 \quad \text{(B-1)}$$

$$Si(OC_2H_5)_4 + H_2O \Leftrightarrow Si(OH)(OC_2H_5)_3 + C_2H_5OH \quad \text{(B-2)}$$

$$Si(OH)(OC_2H_5)_3 + Si(OC_2H_5)_4 \Leftrightarrow O(Si(OC_2H_5)_3)_2 + C_2H_5OH \quad \text{(B-3)}$$

$$2\ Si(OH)(OC_2H_5)_3 \Leftrightarrow O(Si(OC_2H_5)_3)_2 + H_2O \quad \text{(B-4)}$$

and the heterogeneous reactions are

$$Si(OC_2H_5)_4 + SiG_3(OH) \Leftrightarrow SiO_2(D) + SiGE_3 + C_2H_5OH \quad \text{(B-5)}$$

$$SiG_3E \Leftrightarrow SiG_3(OH) + C_2H_4 \quad \text{(B-6)}$$

$$SiG(OH)E_2 \Leftrightarrow SiG(OH)_2E + C_2H_4 \quad \text{(B-7)}$$

$$SiGE_3 \Leftrightarrow SiG(OH)E_2 + C_2H_4 \quad \text{(B-8)}$$

$$SiG(OH)_2E \Leftrightarrow SiG_3(OH) + C_2H_5OH \quad \text{(B-9)}$$

$$SiG(OH)E_2 \Leftrightarrow SiGE_3 + C_2H_5OH \quad \text{(B-10)}$$

$$SiG(OH)_2E \Leftrightarrow SiG_3E + H_2O \quad \text{(B-11)}$$

$$Si(OH)(OC_2H_5)_3 + SiG_3(OH) \Leftrightarrow SiO_2(D) + SiGE_3 + H_2O \quad \text{(B-12)}$$

References

1. Juan C. Rey, Junling Li, Victor Boksha, D. Adalsteinsson, J. A. Sethian, Solid State Technology **41**, 77 (1998).
2. EVOLVE is a deposition, etch, and thin film flow simulator, developed under the direction of Timothy S. Cale. Version 5.0b released in November, 1998.
4. R. J. Kee, F. M. Rupley, J. A. Miller, Sandia Report SAND89-8009B, Sandia National Laboratories, Livermore, CA (1992).
5. Licenses available from Reaction Design, 11436 Sorrento Valley Road, San Diego, CA 92121, (619)550-1920, dhk@ReactionDesign.com.
6. R. M. Levin and K. Evans-Lutterodt, J. Vac. Sci. Technol. B **1**, 54 (1983).
7. F. S. Becker, D. Pawlik, H. Anzinger, and A. Spitzer, J. Vac. Sci. Technol. B **5**, 1555 (1987).
8. Gregory B. Raupp, Frank A. Shemansky, and Timothy S. Cale, J. Vac. Sci. Technol. B **10**, 2422 (1992).
9. Tetsuji Soritä, Satoru Shiga, Kazuyuki Ikuta, Yasuyuki Egashira, and Hiroshi Komiyama, J. Electrochem. Soc. **140**, 2952 (1993).
10. M. M. IslamRaja, C. Chang, J. P. McVittie, M. A. Cappelli, and K. C. Saraswat, J. Vac. Sci. Technol. B **11**, 720 (1993).
11. Michael E. Coltrin, Pauline Ho, Harry K. Moffat, and Richard J. Buss, submitted to Thin Solid Films.
12. Pauline Ho, Carl F. Melius, J. Phys. Chem. **99**, 2166 (1995).
13. E. Meeks, H. K. Moffat, J. F. Grcar, and R. J. Kee, "AURORA: A Fortran Program for Modeling Well Stirred Plasma and Thermal Reactors with Gas and Surface Reactions," Sandia National Laboratories Report SAND96-8218 (1996).
14. Seshu B. Desu, J. Am. Ceram. Soc. **73**, 1615 (1989).
15. J. F. Grcar and W. G. Houf, Sandia National Laboratories Report SAND93-8461 (1993).
16. A. Salinger, K. Devine, G. Hennigan, H. Moffat, S. Hutchinson, and J. Shadid, "MPSalsa: A Finite Element Computer Program for Reacting Flow Problems," Sandia National Laboratories Report, SAND96-2331 (1996).
17. R. Walker, private communication, 1998.
18. William H. Press,Saul A. Teukolsky, William T. Vetterling, and Brian P. Flannery, Numerical Recipes in C, 2nd ed.(Cambridge, 1992), p. 408.
19. Pauline Ho, Michael E. Coltrin, private communication, 1999.

Figures

Figure 1 Reactions on the SiO_2 surface according to the SNL mechanism[11]. Surface species are underlined, gasses appear beside the arrows representing their reactions, and the formula numbers in Appendix B are given in parentheses.

Figure 2 The gas temperature in the experiment reported in Raupp *et al.*[8], as simulated by MPSalsa on a 2-D, axisymmetric mesh. The small SiO_2 sample, heated to 1023 K, creates a plume of hot gas in the 300 K TEOS flow, which is from bottom to top. The radius of the inlet is 2.54 cm.

Figure 3 A close-up of the MPSalsa simulation of the TEOS mole fraction near the sample. Very little TEOS was converted to the reactive $Si(OH)(OC_2H_5)_3$, yet $Si(OH)(OC_2H_5)_3$ contributed 20% of the deposition rate, according to MPSalsa. The radius of the sample is 0.066 cm.

Figure 4 Step coverage simulated over an AR=3.5 trench for the experiment reported in Raupp *et al.*[8]. The SNL mechanism as proposed predicts an overly conformal profile (a), but using the calibrated parameter values from Table V it predicts a less conformal profile (b), more consistent with observation.

Figure 5 Residence time effects on gas composition and deposition rate. Two representative cases are designated as short (6.7 ms) and long (372 ms) residence time. Residence time is inversely proportional to flow rate, but the changing composition of the gas precludes a simple relationship. The species are $Si(OC_2H_5)_4$ (Å), $Si(OH)(OC_2H_5)_3$ (Ç), $O(Si(OC_2H_5)_3)_2$ (G), C_2H_4 (E), H_2O (S), and C_2H_5OH (2).

Figure 6 Residence time effects on surface species site fractions. The species are $SiG_3(OH)$ (B), SiG_3E (F), $SiG(OH)_2E$ (H), $SiG(OH)E_2$ (J), and $SiGE_3$ (P).

Figure 7 Residence time effects on deposition rate on the initial AR = 5 trench. The uniform film thickness seen at long residence time (a) becomes nonuniform for short residence time (b).

Figure 8 Residence time effects on the gas fluxes on the trench profile, normalized to the commonest species in each case. The flux is dominated by $Si(OC_2H_5)_4$ (Å), $Si(OH)(OC_2H_5)_3$ (Ç), and C_2H_4 (E), which impinge uniformly on the feature profile. But while the fluxes of H_2O (S), and C_2H_5OH (2) remain uniform at long residence time (a), at short residence time (b) they show elevated levels in the trench, where the surface to volume ratio is highest, signifying one or both are inhibiting the deposition rate.

Figure 9 Residence time effects on the surface species' site fractions on the trench profile. The uniform fractions at long residence time (a) become nonuniform at short residence time (b). The species are $SiG_3(OH)$ (B), SiG_3E (F), $SiG(OH)_2E$ (H), $SiG(OH)E_2$ (J), and $SiGE_3$ (P).

Figure 10 Residence time effects on the reaction rates on the trench profile. The rate for (B-5) is of order 10^{-6}. All reactions dip slightly within the feature at long residence time (a), while (B-5) behaves contrary to the more pronounced dip at short residence time (b). This shows that the competing (B-12) is rate limiting in the trench at short residence time. The reaction symbols are (B-5) R, (B-6) O, (B-7)Q, (B-8)@, (B-9) D, (B-10)2, (B-11) >, and (B-12) I.

Figure 11 Residence time effects on the effective sticking probability on the trench profile: long residence time (a); short residence time (b): $Si(OC_2H_5)_4$ (Å), $Si(OH)(OC_2H_5)_3$ (Ç), $O(Si(OC_2H_5)_3)_2$ (G), C_2H_4 (E), H_2O (S), and C_2H_5OH (2).

Figure 12 (a) The reaction rates over an AR=3.5 trench for the conditions of Ref. 8 using the SNL mechanism with the original parameter values. (b) The rates using the calibrated parameter values. The reaction symbols are (B-5) R, (B-6)O, (B-7)Q, (B-8)@, (B-9)D, (B-10)2, (B-11) >, and (B-12)I.

Tables

Table I Gas and surface species fractions from the MPSalsa simulation of Raupp *et al.*'s experiment[8].

Gas Species	Mole Fraction	Surface Species	Site Fraction
$Si(OC_2H_5)_4$	0.9999	$SiG_3(OH)$	0.993
$Si(OH)(OC_2H_5)_3$	2.08×10^{-5}	SiG_3E	4.48×10^{-3}
C_2H_5OH	3.33×10^{-5}	$SiG(OH)_2E$	1.42×10^{-4}
C_2H_4	4.21×10^{-5}	$SiG(OH)E_2$	7.30×10^{-4}
H_2O	3.85×10^{-6}	$SiGE_3$	1.74×10^{-3}

Table II Parameters for the well-mixed reactor in residence time simulations.

Parameter	Value
Gas Temperature (K)	1023
Surface Temperature (K)	1023
Flow Rate (sccm)	11.6, 1000
Residence Time (ms)	372, 6.7
Pressure (Torr)	1.0
Reactor Volume (cm^3)	300
Reactor Surface Area (cm^2)	2.5
Inlet Gas Composition	100% TEOS

Table III Step coverages and deposition rate over an AR=3.5 trench by experiment and the SNL mechanism before and after calibration.

Case	sidewall	bottom	minimum	Dep. Rate (Å/min)
Raupp *et al.*[8]	56%	33%	•33%	35
SNL (Uncalibrated)	91%	96%	88%	100
SNL (Calibrated)	49%	41%	38%	122

Table V Reaction mechanism parameters calibrated to the step coverage in the experiment reported in Raupp *et al.*[8].

Parameter	Uncalibrated	Calibrated
$G/R(SiG_3(OH))$	-1.06×10^5	-9.25×10^4
$G/R(SiG_3E)$	-1.18×10^5	-1.83×10^5
$G/R(SiG(OH)_2E)$	-1.55×10^5	-1.73×10^5
$G/R(SiG(OH)E_2)$	-1.67×10^5	-1.58×10^5
$G/R(SiGE_3)$	-1.82×10^5	-1.65×10^5
k_f(B-6) -- A	1.70×10^{12}	9.27×10^{11}
k_f(B-7) -- A	3.40×10^{12}	1.85×10^{12}
k_f(B-8) -- A	5.10×10^{12}	2.78×10^{12}
k_f(B-9) -- A	2.00×10^{12}	4.07×10^{8}
k_f(B-10) -- A	2.00×10^{12}	7.31×10^{8}
k_f(B-11) -- A	2.00×10^{12}	3.76×10^{11}
k_f(B-12) -- A	20.0	46.0

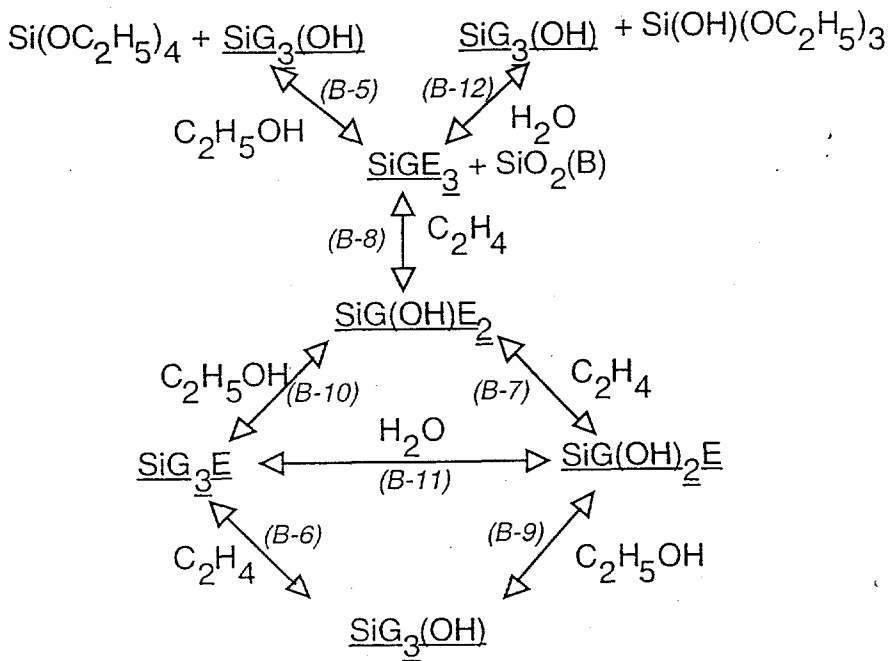

Figure 1 A. H. Labun, H. K. Moffat, T. S. Cale

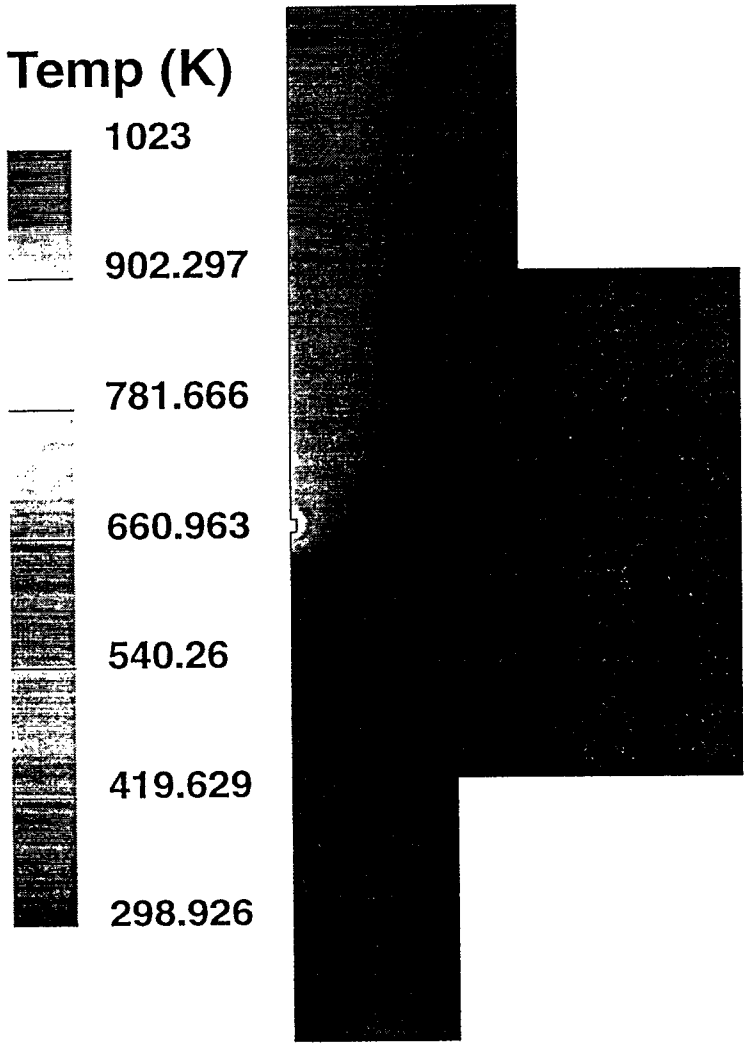

Figure 2 A. H. Labun, H. K. Moffat, T. S. Cale

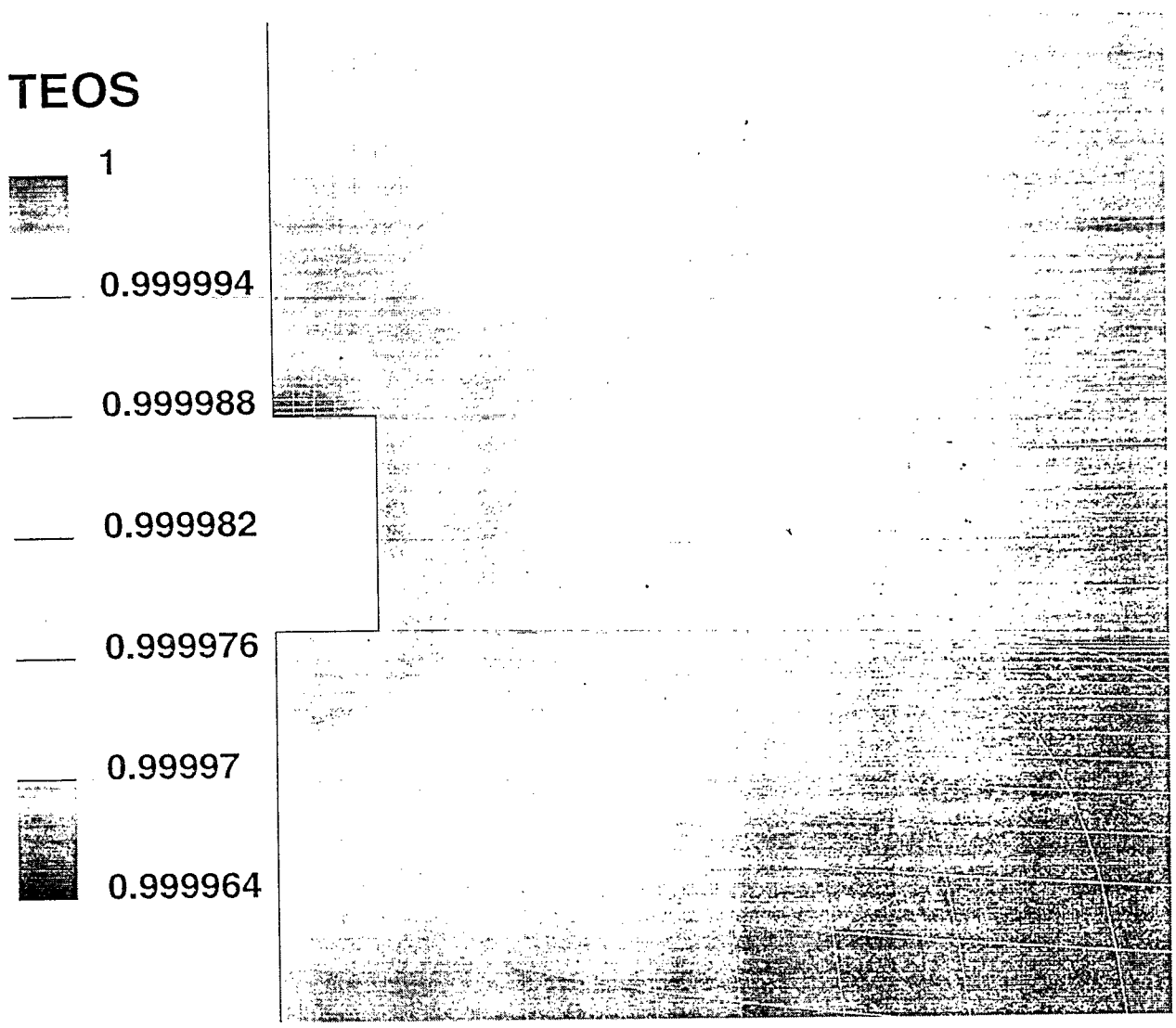

Figure 3 A. H. Labun, H. K. Moffat, T. S. Cale

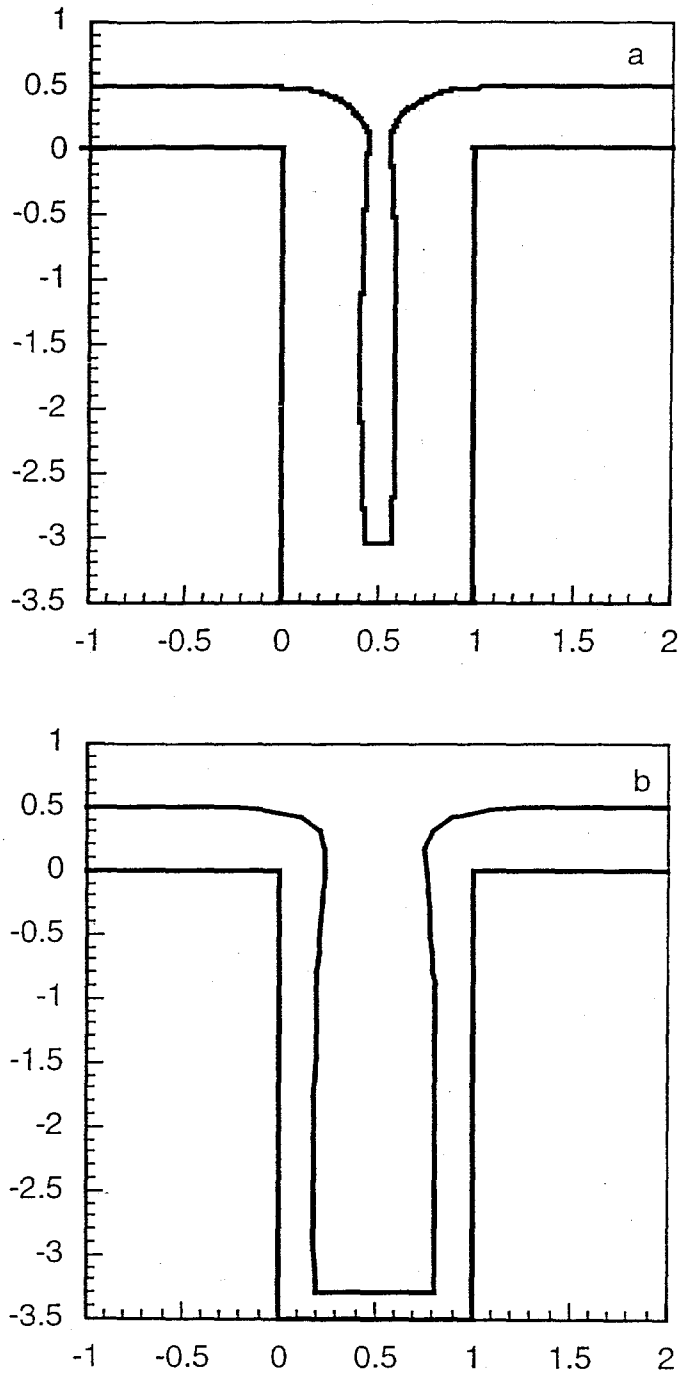

Figure 4 A. H. Labun, H. K. Moffat, T. S. Cale

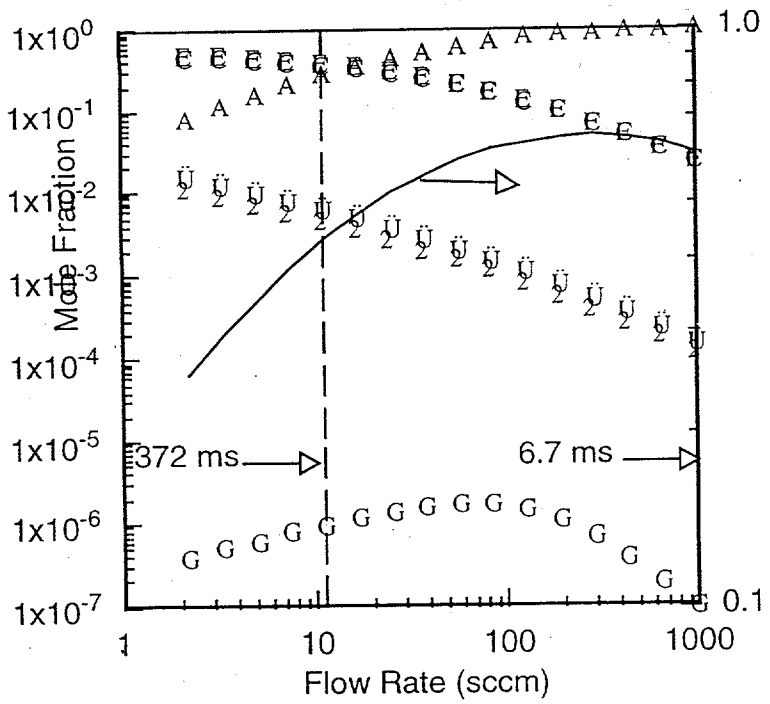

Figure 5 A. H. Labun, H. K. Moffat, T. S. Cale

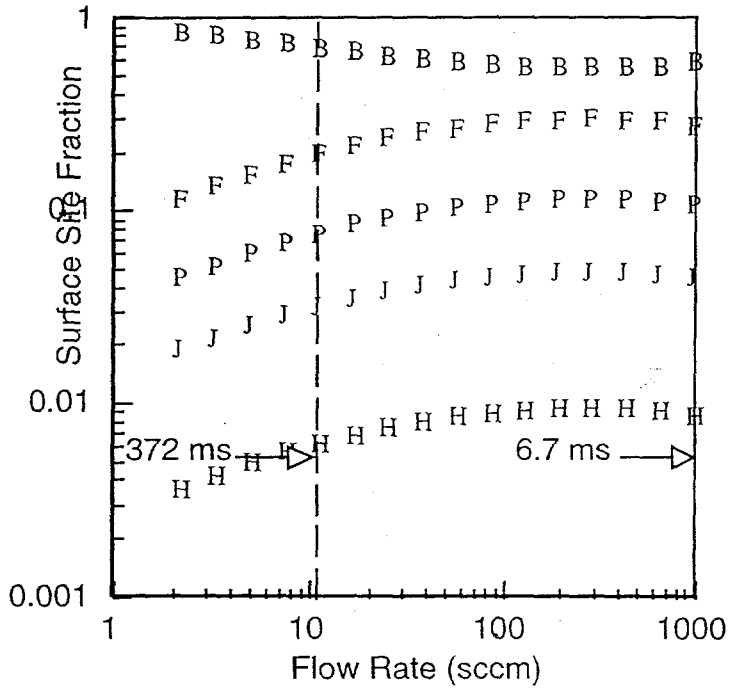

Figure 6 A. H. Labun, H. K. Moffat, T. S. Cale

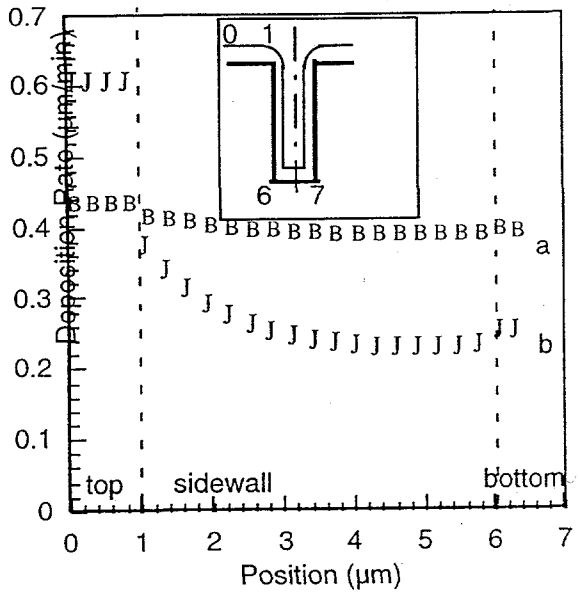

Figure 7 A. H. Labun, H. K. Moffat, T. S. Cale

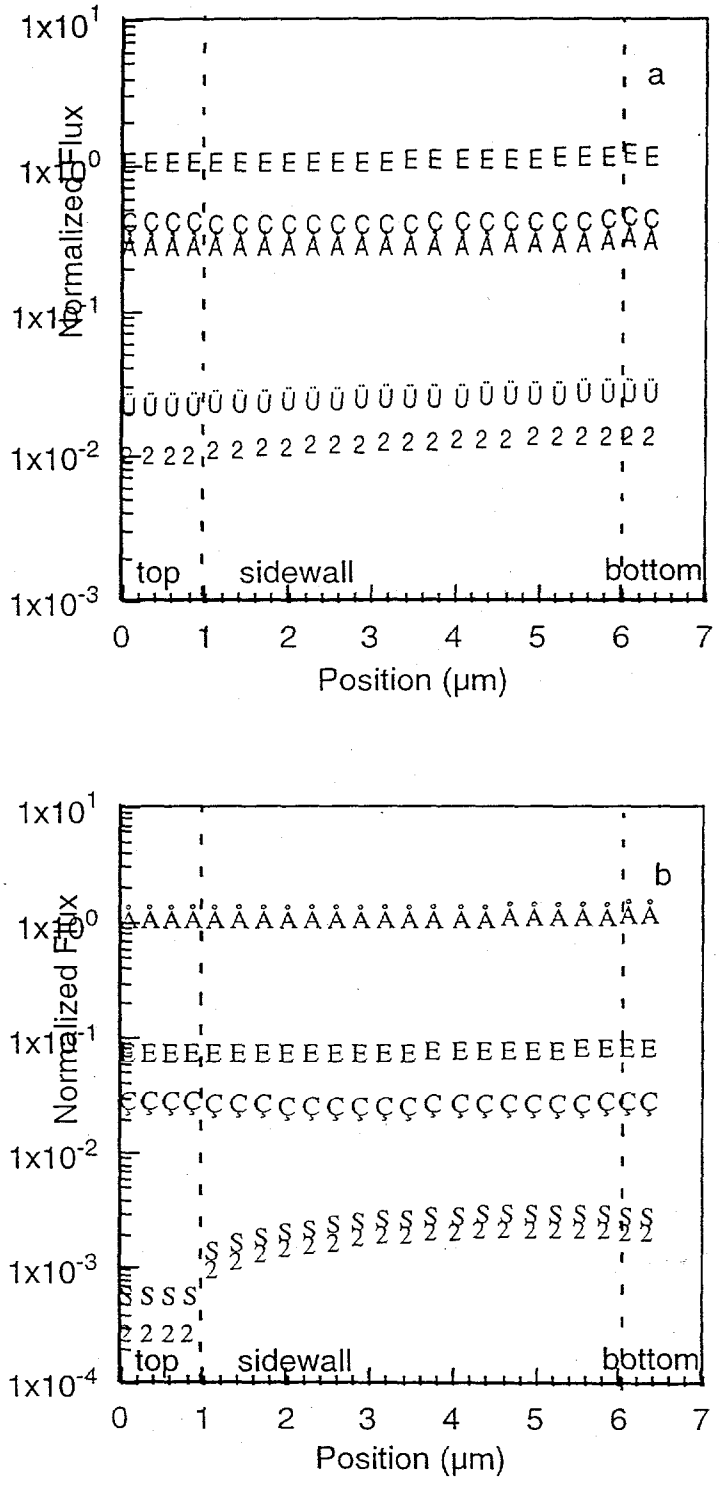

Figure 8 A. H. Labun, H. K. Moffat, T. S. Cale

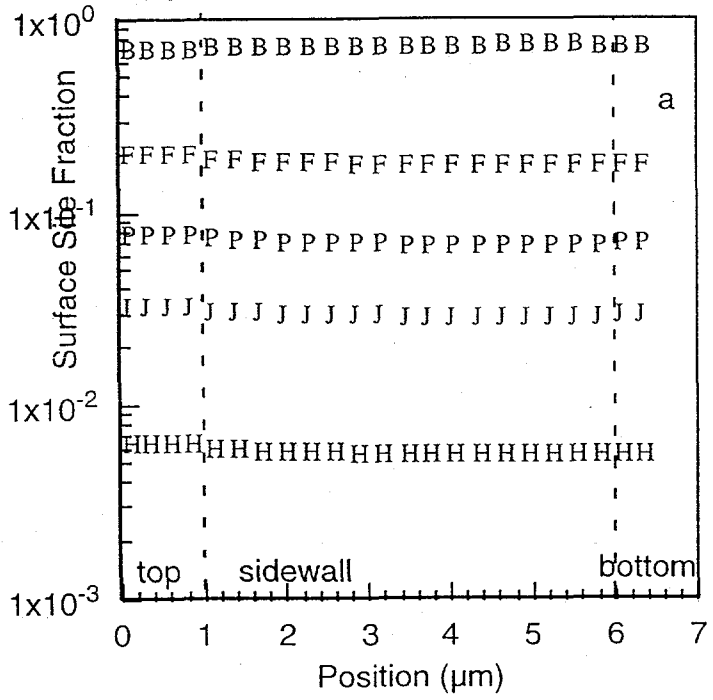

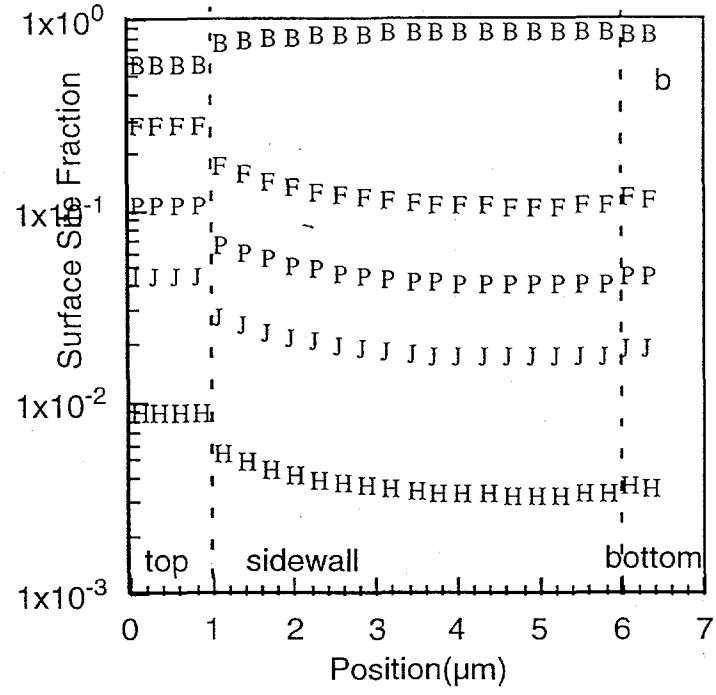

Figure 9 A. H. Labun, H. K. Moffat, T. S. Cale

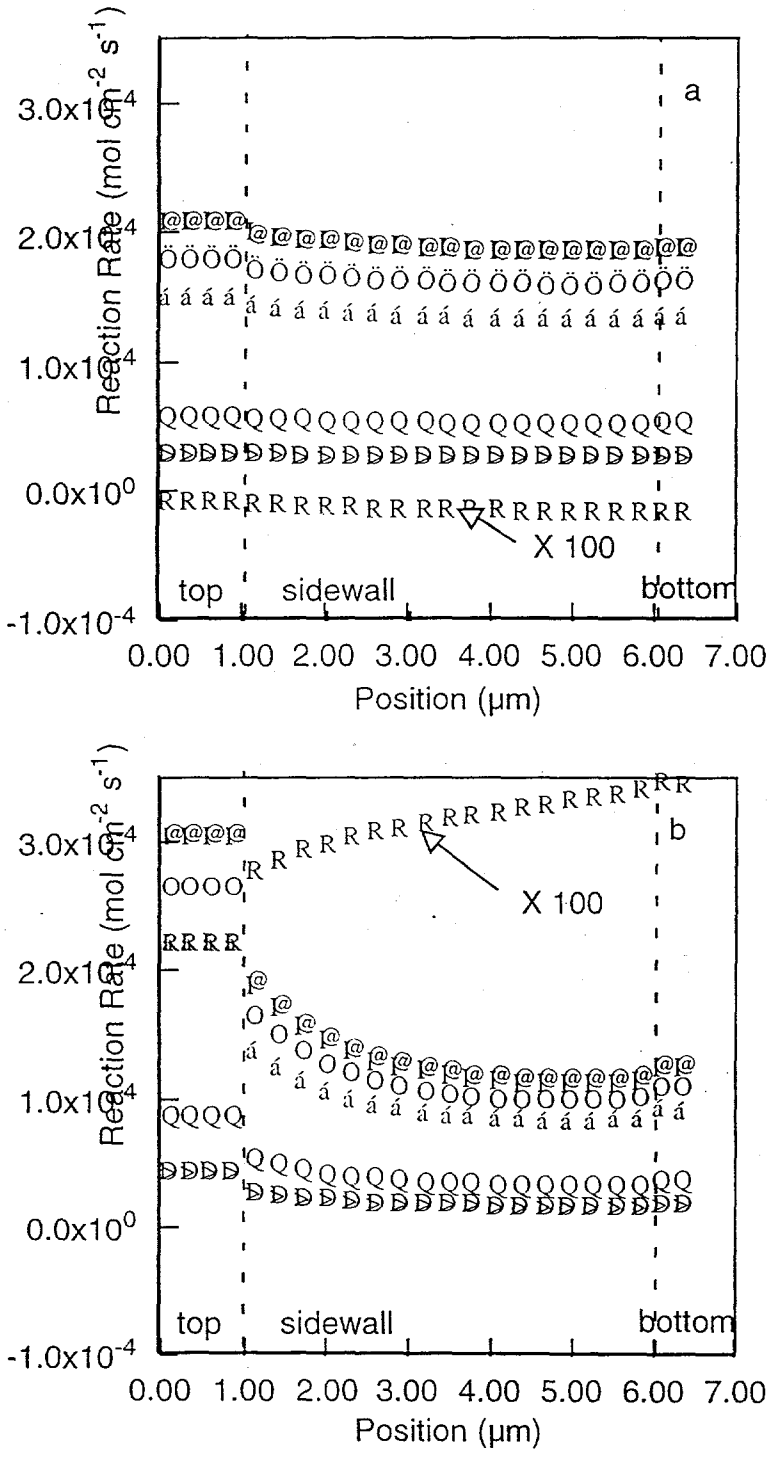

Figure 10 A. H. Labun, H. K. Moffat, T. S. Cale

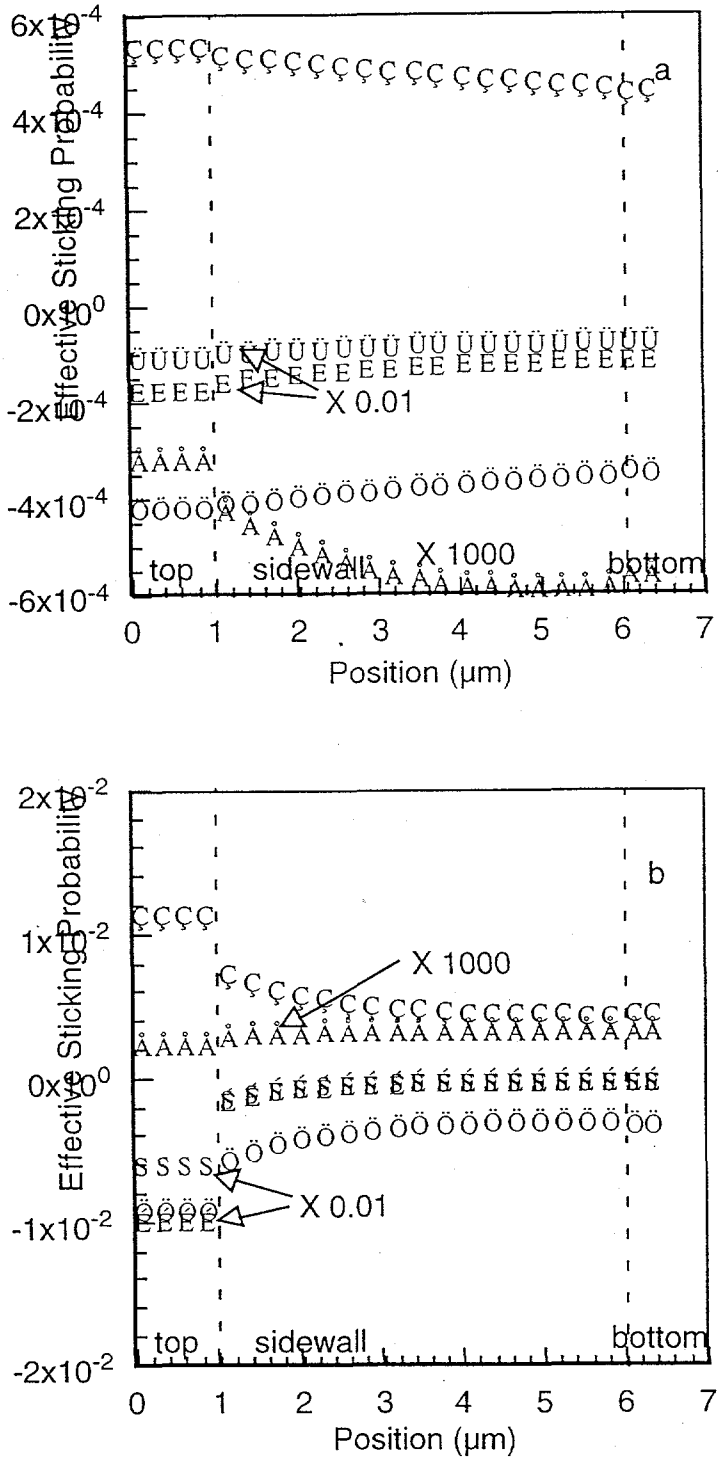

Figure 11 A. H. Labun, H. K. Moffat, T. S. Cale

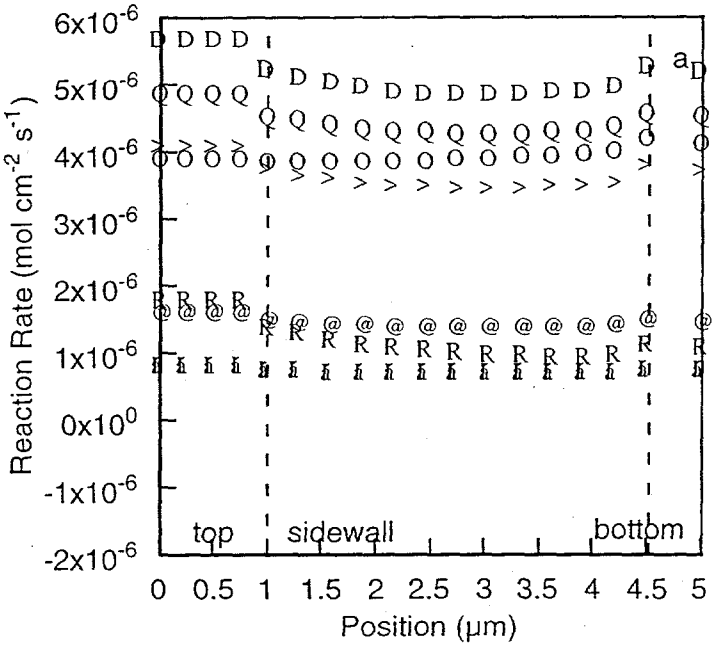

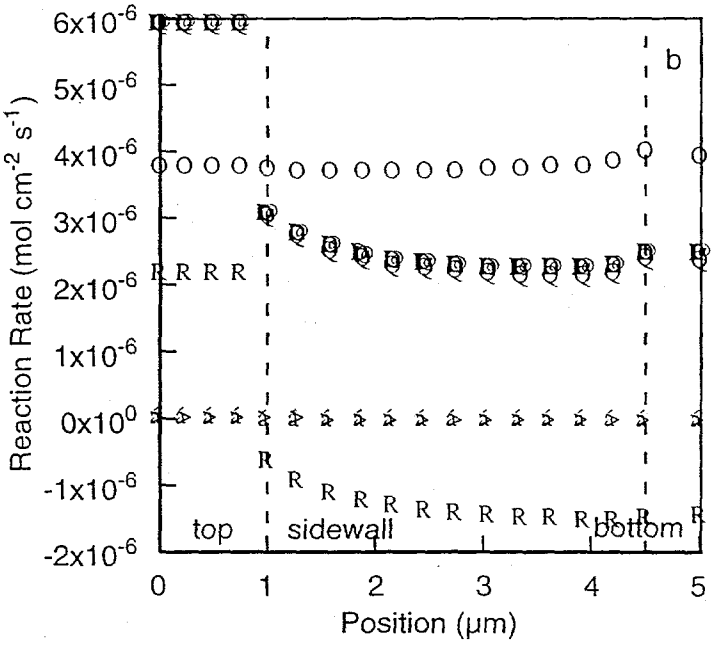

Figure 12 A. H. Labun, H. K. Moffat, T. S. Cale

[1] Juan C. Rey, Junling Li, Victor Boksha, D. Adalsteinsson, J. A. Sethian, Solid State Technology **41**, 77 (1998).
[2] EVOLVE is a deposition, etch, and thin film flow simulator, developed under the direction of Timothy S. Cale. Version 5.0b released in November, 1998.
[3] R. J. Kee, F. M. Rupley, J. A. Miller, Sandia Report SAND89-8009B, Sandia National Laboratories, Livermore, CA (1992).
[4] M. E. Coltrin, R. J. Kee, F. M. Rupley, Sandia Report SAND90-8003C, Sandia National Laboratories, Livermore, CA (1994).
[5] Licenses available from Reaction Design, 11436 Sorrento Valley Road, San Diego, CA 92121, (619)550-1920, dhk@ReactionDesign.com.
[6] R. M. Levin and K. Evans-Lutterodt, J. Vac. Sci. Technol. B **1**, 54 (1983).
[7] F. S. Becker, D. Pawlik, H. Anzinger, and A. Spitzer, J. Vac. Sci. Technol. B **5**, 1555 (1987).
[8] Gregory B. Raupp, Frank A. Shemansky, and Timothy S. Cale, J. Vac. Sci. Technol. B **10**, 2422 (1992).
[9] Tetsuji Sorita, Satoru Shiga, Kazuyuki Ikuta, Yasuyuki Egashira, and Hiroshi Komiyama, J. Electrochem. Soc. **140**, 2952 (1993).
[10] M. M. IslamRaja, C. Chang, J. P. McVittie, M. A. Cappelli, and K. C. Saraswat, J. Vac. Sci. Technol. B **11**, 720 (1993).
[11] Michael E. Coltrin, Pauline Ho, Harry K. Moffat, and Richard J. Buss, submitted to Thin Solid Films.
[12] Pauline Ho, Carl F. Melius, J. Phys. Chem. **99**, 2166 (1995).
[13] Pauline Ho, Carl F. Melius, J. Phys. Chem. **99**, 2166 (1995).
[14] E. Meeks, H. K. Moffat, J. F. Grcar, and R. J. Kee, Sandia National Laboratories Report SAND96-8218 (1996).
[15] Seshu B. Desu, J. Am. Ceram. Soc. **73**, 1615 (1989).
[16] J. F. Grcar and W. G. Houf, Sandia National Laboratories Report SAND93-8461 (1993).
[17] A. Salinger, K. Devine, G. Hennigan, H. Moffat, S. Hutchinson, and J. Shadid, MPSalsa: A Finite Element Computer Program for Reacting Flow Problems, Sandia National Laboratories Report, SAND96-2331 (1996).
[18] R. Walker, private communication, 1998.
[19] William H. Press,Saul A. Teukolsky, William T. Vetterling, and Brian P. Flannery, Numerical Recipes in C, 2nd ed.(Cambridge, 1992), p. 408.
[20] Pauline Ho, Michael E. Coltrin, private communication, 1999.